



UNIVERSITY OF LEEDS

This is a repository copy of *Impact of water vapour and carbon dioxide on surface composition of C3A polymorphs studied by X-ray photoelectron spectroscopy*.

White Rose Research Online URL for this paper:
<http://eprints.whiterose.ac.uk/84269/>

Version: Accepted Version

Article:

Dubina, E, Plank, J and Black, L (2015) Impact of water vapour and carbon dioxide on surface composition of C3A polymorphs studied by X-ray photoelectron spectroscopy. *Cement and Concrete Research*, 73. 36 - 41. ISSN 0008-8846

<https://doi.org/10.1016/j.cemconres.2015.02.026>

(c) 2015, Elsevier. Licensed under the Creative Commons Attribution-NonCommercial-NoDerivatives 4.0 International
<http://creativecommons.org/licenses/by-nc-nd/4.0/>

Reuse

Unless indicated otherwise, fulltext items are protected by copyright with all rights reserved. The copyright exception in section 29 of the Copyright, Designs and Patents Act 1988 allows the making of a single copy solely for the purpose of non-commercial research or private study within the limits of fair dealing. The publisher or other rights-holder may allow further reproduction and re-use of this version - refer to the White Rose Research Online record for this item. Where records identify the publisher as the copyright holder, users can verify any specific terms of use on the publisher's website.

Takedown

If you consider content in White Rose Research Online to be in breach of UK law, please notify us by emailing eprints@whiterose.ac.uk including the URL of the record and the reason for the withdrawal request.



eprints@whiterose.ac.uk
<https://eprints.whiterose.ac.uk/>

1 **Date: 27.11.2014**

2

3 **Impact of Water Vapour and Carbon Dioxide on Surface Composition of**
4 **C₃A Polymorphs Studied by X-Ray Photoelectron Spectroscopy**

5

6 Dubina E.¹, Plank J.¹, , Black L.^{2*}

7

8

9

10 ¹Technische Universität München, Lehrstuhl für Bauchemie, Lichtenbergstr. 4, 85747
11 Garching bei München, Germany

12

13 ²Institute for Resilient Infrastructure, School of Civil Engineering, University of Leeds, Leeds,
14 LS2 9JT, UK

15

16

17

18

19

20

21 **Number of Words: 3,820 - main text only (without references)**

22 **Number of Figures: 7**

23 **Number of Tables: 4**

24

25

* Corresponding author: Email l.black@leeds.ac.uk (Leon Black) Tel + 44 – 113 – 343 – 2283,
Fax + 44 – 113 – 343 – 2265

26
27
28
29
30
31
32
33
34
35
36
37
38
39
40
41
42
43
44
45
46
47
48
49
50
51

Abstract

The surface specific analytical method, x-ray photoelectron spectroscopy (XPS), has been used to study the effects of water vapour and CO₂ on the cubic and orthorhombic polymorphs of C₃A. Significant differences between the two polymorphs were observed in the XPS spectra. Upon exposure to water vapour, both polymorphs produced C₄AH₁₃ on their surfaces. Additionally, the sodium-doped o-C₃A developed NaOH and traces of C₃AH₆ on its surface. Subsequent carbonation yielded mono carboaluminate on both polymorphs. Large amounts of Na₂CO₃ also formed on the surface of o-C₃A as a result of carbonation of NaOH. Furthermore, the extent of carbonation was much more pronounced for o-C₃A₀ than for c-C₃A.

106 Words

Key words: Ca₃Al₂O₆ polymorphs (D), prehydration, carbonation (C), X-ray photoelectron spectroscopy

52 **1. Introduction**

53 Tricalcium aluminate (C_3A) constitutes $\sim 2 - 12$ wt. % of Portland cement clinker. In
54 industrial cement, C_3A usually occurs as one of two polymorphs; cubic or orthorhombic. It is
55 well known that C_3A can incorporate a large number of minor and trace elements into its
56 crystal structure [1 – 4]. The impact of these elements on the crystal structure as well as the
57 hydration behaviour and kinetics has been thoroughly discussed in previous works [5 – 9].

58

59 Among those impurities, alkalis (K_2O , Na_2O) appear to be the most important modifying
60 oxides. These oxides are able to change the crystal system of C_3A from cubic to orthorhombic
61 and to monoclinic [8], and sodium oxide plays a significant role in stabilising different
62 modifications of C_3A . The structure of pure, undoped, cubic C_3A has been determined by
63 Mondal and Jeffery. They also discussed the solid solutions of the Na_2O-C_3A series [10].
64 Isomorphic substitution of calcium by sodium in solid solutions formed at $1250\text{ }^\circ\text{C}$ leads to
65 crystallisation into the cubic polymorph at Na_2O contents of $0 - 2.5\%$ (by mass), the
66 orthorhombic polymorph at $3.5 - 4.2\%$ Na_2O , and the monoclinic polymorph at $> 4.2\%$
67 Na_2O [11].

68

69 C_3A is the most reactive phase within cement clinker. In the absence of soluble sulphates, it
70 instantaneously forms massive amounts of hydration products, mainly calcium aluminate
71 hydrates (C-A-H phases of different stoichiometric compositions). Owing to this high
72 reactivity, C_3A can react with atmospheric water vapour during storage; a phenomenon
73 known as prehydration of cement [8,12]. It has been demonstrated that, of all the cement
74 constituents, C_3A reacts preferably with water vapour when cement is prehydrated [13], with
75 an impact on the eventual setting behaviour of the cement [14]. However, the cubic and
76 orthorhombic C_3A polymorphs exhibit different behaviours when exposed to water vapour

77 [8]. For orthorhombic C_3A , the onset point at which water sorption starts to occur lies at 55 %
78 relative humidity (RH), compared to 80 % RH for cubic C_3A [15].

79
80 Prehydration is predominantly a surface reaction, hence common bulk analysis methods such
81 as x-ray diffraction are of limited value. Instead, surface specific analytical techniques, such
82 as X-ray photoelectron spectroscopy (XPS), may be used to provide information on the
83 composition and speciation of the prehydrated surface, without interference from the
84 unaffected bulk material [16]. In XPS, the sample is irradiated with x-rays in order to provoke
85 the photoelectric effect, with the energy of the emitted photoelectrons being characteristic of
86 the element from which they are emitted and the chemical state of the element. The low
87 energy of the photoelectrons ensures that only those emitted from the surface of the irradiated
88 sample are detected, Consequently, XPS allows the analysis of surface layers typically 1 to 10
89 nm thick, with all elements bar hydrogen being capable of identification [17].

90
91 In the present study, the impact of initial exposure of C_3A to moisture, followed by interaction
92 with atmospheric CO_2 , has been investigated by XPS. Furthermore, the influence of Na_2O ,
93 present in the orthorhombic modification of C_3A , on these processes was studied.

94

95 **2. Materials and Methods**

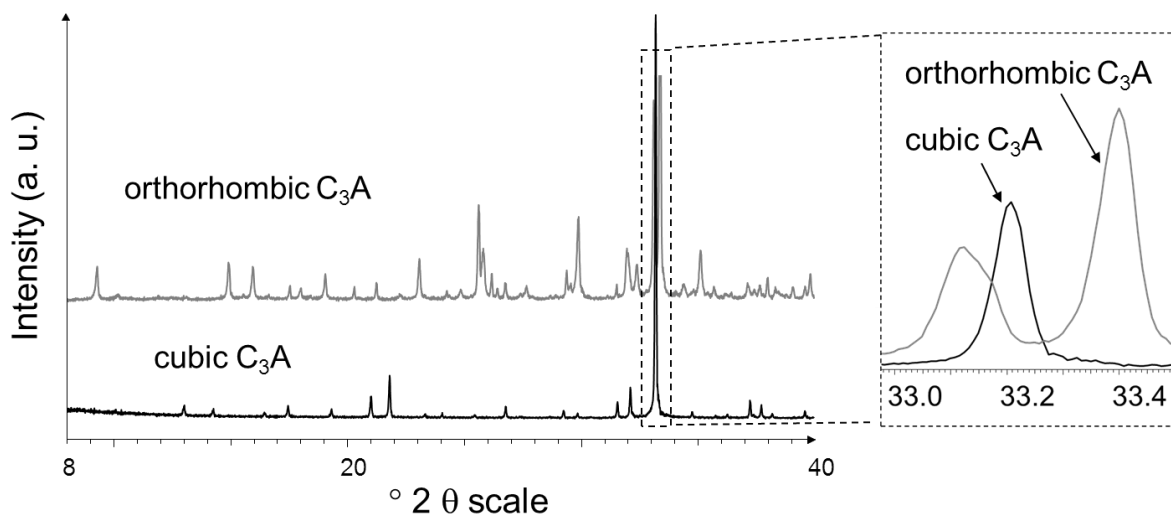
96 **2.1 Synthesis of C_3A polymorphs**

97 Pure, undoped cubic C_3A and orthorhombic C_3A doped with 4 wt. % Na_2O were synthesised
98 according to the literature [16], using calcium carbonate and aluminium oxide as starting
99 materials. Sodium nitrate was used as the Na_2O source in the preparation of orthorhombic
100 C_3A . The samples, sintered at 1450 °C for 4 hours, were removed from the oven, allowed to
101 cool in air for 3 minutes in covered Pt crucibles and then immediately placed in the cup of a
102 steel ball mill (Planetary Mono Mill PULVERISETTE 6 classic line, Fritsch, Idar-Oberstein,

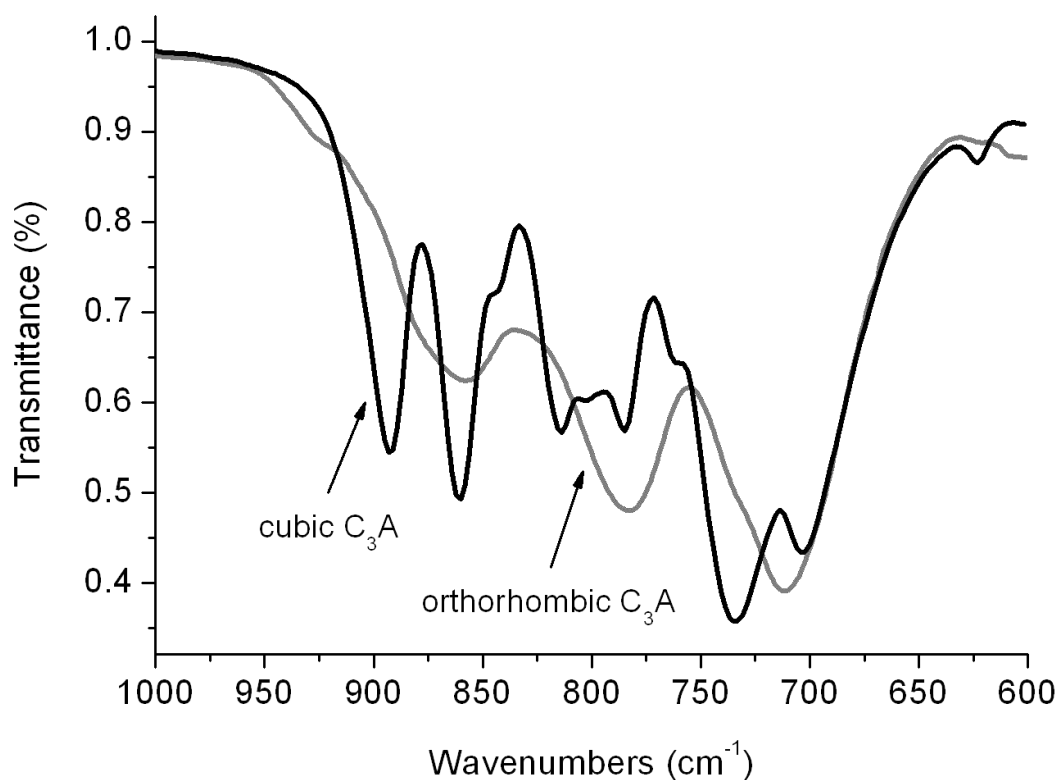
103 Germany). Grinding was performed in air at 250 rpm for 10 minutes at a temperature of 21 °C
104 without the addition of a grinding agent. The ground samples were stored in sealed 20 mL
105 glass bottles placed in a vacuum desiccator.

106
107 According to quantitative X-Ray diffraction (XRD) analysis of freshly prepared samples, the
108 C_3A phases were 99 ± 0.5 wt. % pure. Their XRD patterns are presented in **Figure 1**. FTIR-
109 ATR spectra of the synthesised C_3A samples further confirmed their phase purity. **Figure 2**
110 shows the characteristic differences between the two polymorphs: with a reduction in the
111 number of IR bands for orthorhombic C_3A , as a result of altered symmetry of the Al_6O_{18} ring
112 ($C_3 \rightarrow C_i$). Furthermore, partial substitution of Ca^{2+} by Na^+ induces disorder in the structure
113 and thus broadening of the bands [2].

114



115
116 **Fig. 1.** XRD patterns of cubic and orthorhombic C_3A phases as prepared, shown over the
117 range 8 – 40° 2θ



118

119 **Fig. 2.** FTIR-ATR spectra of cubic and orthorhombic C_3A phases as prepared, shown over the
 120 range 600 – 1000 cm^{-1}

121

122 The surface of orthorhombic C_3A was investigated by scanning electron microscopy (SEM)
 123 using a FEI XL 30 FEG microscope equipped with a large field detector under low vacuum
 124 conditions (1 mbar H_2O pressure, corresponding to ~ 4 % RH at room temperature).

125

126 2.2 Water and CO_2 exposure of samples

127 200 mg of powdered C_3A were pressed into pellets ($d = 13$ mm) at a pressure of 50 N/mm^2
 128 using a hydraulic press. The pellets of cubic and orthorhombic C_3A were then refired at
 129 1350 $^{\circ}C$ for 3 h (c- C_3A) or 20 minutes (o- C_3A) to achieve complete dehydration and
 130 decarbonation.

131

132 However, preliminary XPS analysis of the C_3A pellets still showed evidence of slight
 133 carbonation. Thus, to obtain a completely pristine surface, all samples were etched by argon

134 ion bombardment under vacuum in the spectrometer, prior to any exposure to water vapour
135 and CO₂.

136

137 Each sample was cleaned by ion bombardment in the spectrometer and then subjected to three
138 different exposure cycles. Pellets were placed in a nitrogen gas filled desiccator which was
139 placed in a glove box. The relative humidity over the samples was adjusted to 85 % using a
140 saturated potassium chloride solution within the desiccator [18]. Samples were initially
141 exposed for 4 hours, and then analysed. Subsequently, the same sample was prehydrated
142 under the same conditions for a further 8 hours before the second analysis. The third and final
143 cycle exposed the previously prehydrated sample to atmospheric conditions, i.e. ambient air
144 containing CO₂, for a further 12 hours. Throughout the rest of the manuscript samples are
145 identified as; 0h, 4h, 12h and 24c, where h and c indicate exposure to humidity or CO₂
146 respectively and the number indicates the duration of exposure.

147

148 **2.3 XPS analysis**

149 Each pellet was stuck onto a double-sided adhesive copper tape and inserted into the vacuum
150 chamber for analysis. The samples were analysed using a SCIENTA ESCA 300 photoelectron
151 spectrometer (located at the National Centre for Electron Spectroscopy and Surface Analysis,
152 NCESS, Daresbury, UK) fitted with a high power rotating anode (8 kW) and a
153 monochromatic Al K_α (hv = 1486.7 eV) X-ray source. The X-ray beam was focused on a
154 6 mm × 0.5 mm area on the sample via a large, seven crystal double focusing
155 monochromator. The Al K_α line profile had a FWHM (full width at half maximum) energy
156 width of 0.26 eV. The detection system consisted of a 300 mm radius hemispherical analyser
157 and a multi-channel detector. The system was operated with 0.8 mm slits and 150 eV pass
158 energy, giving an overall instrument resolution of 0.30 eV ± 0.05 eV FWHM. Because the

159 samples were often extremely good electrical insulators, a flood gun was used to compensate
160 for sample charging.

161
162 Following an initial survey scan, high resolution spectra were recorded for the elements of
163 interest: Na 1s, Ca 2p, O 1s, C 1s, Al 2p. Derived sensitivity factors were applied to convert
164 signal intensities to atomic compositions [19].

165
166 Data were extracted from the spectra via peak fitting using CasaXPS software. A Shirley
167 background was assumed in all cases. Spectra were corrected for charging effects using the
168 adventitious hydrocarbon peak at 284.8 eV binding energy (BE). This peak is ubiquitous due
169 to carbon contamination from the vacuum systems [20]. The presence of inorganic carbon, as
170 carbonate, was always looked for in high-resolution scans.

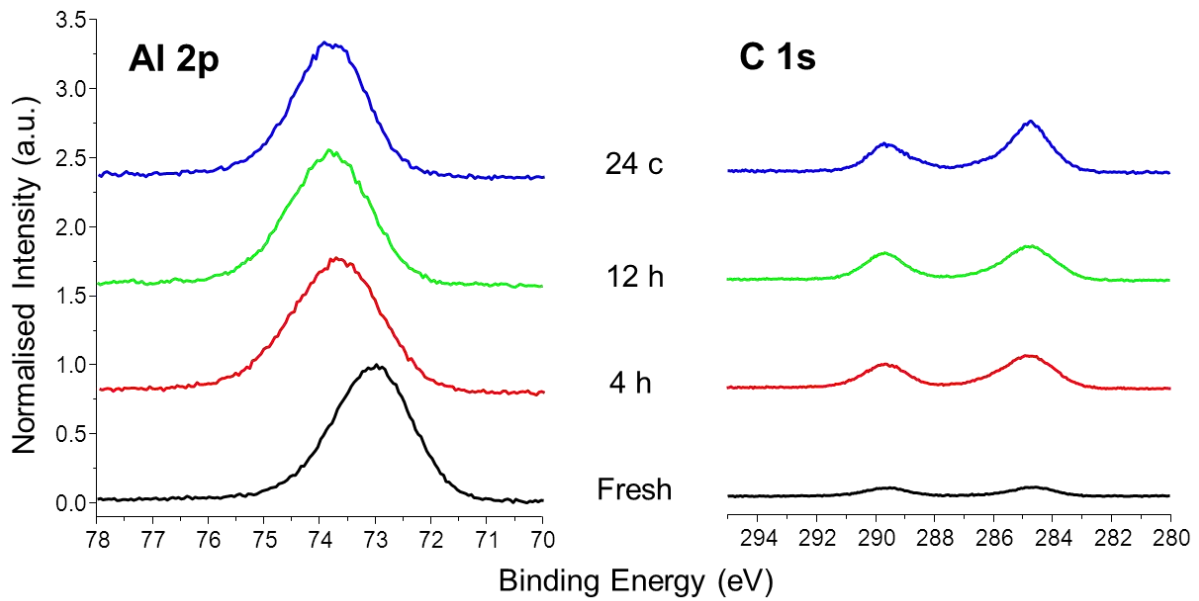
171

172 **3. Results and discussion**

173 **3.1 XPS analysis of fresh C₃A polymorphs**

174 **Figures 3 and 4** show the Al 2p and C 1s XPS spectra obtained from both polymorphs after
175 each exposure. The corresponding binding energies and elemental ratios are tabulated in
176 **Tables 1 – 4**. Note that, for simplicity, quantification assumed that samples were
177 homogeneous with respect to depth.

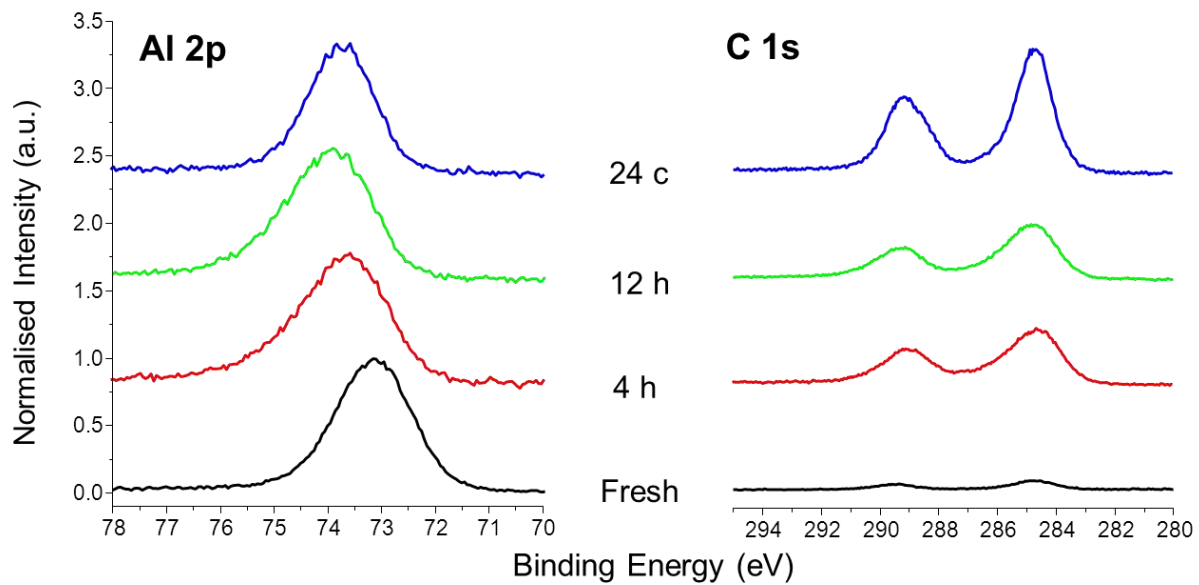
178



179

180 **Fig. 3** XPS spectra of non-doped, cubic C_3A sample, fresh and aged, showing the evolution of
 181 the Al 2p (left) and C 1s (right) peaks upon exposure to water vapour and subsequent
 182 carbonation

183



184

185 **Fig. 4** XPS spectra of Na-doped orthorhombic C_3A sample, fresh and aged, showing the
 186 evolution of the Al 2p (left) and C 1s (right) peaks upon exposure to water vapour and
 187 subsequent carbonation

188

189 **Table 1** Binding energies of fresh and aged cubic C₃A, as obtained by XPS

| Element | Binding energy (eV)* after exposure period/mode | | | |
|----------------------|---|-------|-------|-------|
| | 0 h (fresh) | 4 h | 12 h | 24 c |
| Ca 2p _{2/3} | 346.4 | 347.1 | 347.2 | 347.2 |
| O 1s | 529.7 | 531.2 | 531.3 | 531.3 |
| | 531.4 | 531.7 | 531.7 | 531.7 |
| Al 2p | 72.9 | 73.5 | 73.7 | 73.8 |
| | 73.5 | 74.1 | 74.3 | 74.7 |
| C 1s | 289.7 | 289.7 | 289.7 | 289.6 |

190 * Shifts relative to C 1s = 284.8 eV

191

192 **Table 2** Element ratios and chemical shifts of fresh and aged cubic C₃A, as obtained from
193 XPS analysis

| El. ratios | Element ratios and chemical shifts (eV)* after exposure period/mode | | | |
|-------------------------|---|-------|-------|-------|
| | 0 h (fresh) | 4 h | 12 h | 24 c |
| Ca/Al* | 1.5 | 1.47 | 1.48 | 1.47 |
| C/Ca | 0.07 | 0.17 | 0.19 | 0.3 |
| $\Delta_{\text{Ca-Al}}$ | 273.4 | 273.4 | 273.3 | 273.4 |
| $\Delta_{\text{Ca-C}}$ | 56.8 | 57.4 | 57.5 | 57.6 |

194 *: Values represent normalized ratios based on the assumption that etched sample possesses the
195 ideal composition Ca₃Al₂O₆.
196

197 **Table 3** Binding energies of fresh and aged orthorhombic C₃A derived from XPS analysis

| Element | Binding energy (eV)* after exposure period/mode | | | |
|----------------------|---|--------|--------|--------|
| | 0 h | 4 h | 12 h | 24 c |
| Ca 2p _{2/3} | 346.4 | 346.7 | 347.0 | 346.8 |
| O 1s | 529.8 | 531.0 | 531.2 | 531.2 |
| | 531.7 | 531.8 | 531.9 | 532.7 |
| Al 2p | 73.1 | 73.5 | 73.7 | 73.7 |
| | 74.1 | 74.5 | 74.5 | - |
| Na 1s | 1071.6 | 1071.5 | 1071.5 | 1071.4 |
| | 1072.2 | 1072.3 | 1072.4 | 1072.2 |
| C 1s | 289.6 | 289.3 | 289.2 | 289.3 |

198 * Shifts relative to C 1s = 284.8 eV

199

200 **Table 4** Element ratios and chemical shifts of fresh and aged orthorhombic C₃A, as obtained
201 from XPS analysis

| El. ratios | Element ratios and chemical shifts (eV)* after exposure period /mode | | | |
|-------------------------|--|-------|-------|-------|
| | 0 h (fresh) | 4 h | 12 h | 24 c |
| Ca/Al* | 1.42 | 2.05 | 2.01 | 1.98 |
| Na/Ca* | 0.12 | 0.55 | 0.91 | 2.94 |
| C/Ca | 0.04 | 0.22 | 0.20 | 0.83 |
| Na/C | 0.47 | 0.43 | 0.78 | 0.75 |
| $\Delta_{\text{Ca-Al}}$ | 273.3 | 272.9 | 273.0 | 273.0 |
| $\Delta_{\text{Ca-C}}$ | 56.9 | 57.6 | 57.6 | 57.7 |
| $\Delta_{\text{Na-C}}$ | 782.2 | 782.4 | 782.5 | 782.3 |

202 *: Values represent normalized ratios based on the assumption that etched sample has the ideal
203 composition Ca_{8.5}NaAl₆O₁₈.
204

205
206 The Al 2p spectra for the fresh phases were slightly asymmetrical, due to spin orbit coupling
207 of the Al 2p lines, with the undoped, more calcium-rich, cubic C₃A having a slightly lower
208 binding energy than orthorhombic C₃A (**Figures 3 and 4**). The Al 2p spectra for the fresh
209 samples show two contributions, namely at ~ 72.9 and 73.5 eV for the cubic and at ~ 73.1 and
210 74.0 eV for the orthorhombic C₃A polymorph (**Tables 1 and 3**). The spectra reported here for
211 cubic C₃A are very similar to the binding energy of 73.1 eV reported by Ball et al. [21].
212 Aluminium binding energies are dependent upon the coordination number [22,23]. In both
213 C₃A modifications, Al is always tetrahedrally coordinated and occurs as AlO₄. Six such
214 tetrahedra form an Al₆O₁₈¹⁸⁻ ring in orthorhombic C₃A which becomes deformed upon
215 replacement of Ca²⁺ by the slightly less electronegative Na⁺ in the centre of the Al₆O₁₈¹⁸⁻ ring
216 [24]. Thus, the slight changes in binding energy from cubic to orthorhombic C₃A may be due
217 to the symmetry change (C₃ → C_i) or a change in electronegativity caused by the
218 incorporation of Na₂O into doped C₃A.

219
220 The Ca 2p binding energies for both fresh polymorphs were the same and in good agreement
221 with the value of 346.3 eV obtained by Ball et al. [21]. Unlike the Al 2p spectra, Ca 2p
222 binding energies are less sensitive to changes in composition, e.g. in both calcium aluminate
223 hydrate [21] and calcium silicate hydrate [21, 22] systems. Consequently, spectra would not
224 be expected to change upon replacement of calcium by sodium.

225
226 In addition to the binding energies, changes in the Ca 2p – Al 2p energy separation ($\Delta_{\text{Ca-Al}}$)
227 were determined (**Tables 2 and 4**). In previous studies on calcium silicate hydrates, these
228 values have been shown to provide valuable information related to changes in their chemical
229 structure, in particular the degree of silicate polymerisation in calcium silicate hydrates
230 [20,25]. This approach also overcomes problems due to charging when analysing insulating

231 samples. Here, the incorporation of sodium into the C_3A lattice, with the conversion from
232 cubic to orthorhombic, did not induce changes in polymerisation, but there was a slight
233 reduction in Δ_{Ca-Al} from 273.4 to 273.2 eV, likely as a result of the reduced electronegativity
234 of sodium compared to calcium.

235

236 **3.2 Exposure to water vapour and CO₂**

237 In a previous investigation, there was a distinct difference between the XPS spectra of the
238 surfaces of cubic and orthorhombic C_3A prehydrated in moist air (85 % RH, and including
239 CO₂) for just 1 h [21]. In this study emphasis has been placed on separation of the effects
240 caused by water vapour and carbon dioxide.

241

242 Prehydration under water vapour only (no CO₂ present) was slower than in the previous study
243 where prehydration was performed in moist, CO₂-containing air. Nonetheless, exposure to
244 water vapour led to spectral changes and shift to higher Al 2p binding energies (**Figures 3**
245 **and 4**). Furthermore, the Al 2p spectra broadened upon prehydration and two peaks were
246 required to fit them, signifying a change in the chemical environment of Al, plausibly due to
247 formation of C-A-H phases. An Al 2p binding energy of 73.8 eV has previously been reported
248 for pure C_4AH_{13} [16]. Here, after exposure of both C_3A polymorphs to water vapour for 12 h,
249 a peak could be fitted at ~ 73.7 eV, likely indicative of C_4AH_{13} formation. The second peak in
250 the Al 2p spectra was centred at ~ 74.3 eV for the cubic and at ~ 74.5 eV for the orthorhombic
251 modification. These peaks might be attributable to C_3AH_6 (katoite), as was found by a
252 combination of XRD and XPS in the aforementioned previous study [16].

253

254 Upon exposure to air, i.e. upon carbonation, the Al 2p spectra of both polymorphs showed
255 further changes, with formation of carbonate observed in the C 1s spectra, as indicated by a
256 peak at ~ 289 eV (**Fig 3 and 4**).

257 For the cubic modification, the relative peak areas of the Ca 2p and C 1s spectra (Ca 2p
258 spectra not shown here) suggest a C/Ca ratio of 0.3 (**Table 2**), indicating the formation of
259 calcium monocarboaluminate ($3 \text{ CaO} \cdot \text{Al}_2\text{O}_3 \cdot \text{CaCO}_3 \cdot 11 \text{ H}_2\text{O}$). This is in agreement with
260 the bulk carbonation behaviour of C_3A pastes, as analysed by Raman spectroscopy [26]. The
261 mechanism of the monocarboaluminate formation is based on the reaction of CO_2 with C_4AH_x
262 phases which possesses a disordered layered structure. In this process, the interlayer OH^- is
263 replaced by CO_3^{2-} [27]. The ion exchange stabilises the layered structure and results in
264 shrinkage of the basal spacing from 1.08 nm in C_4AH_{13} to 0.76 nm for the carbonated species
265 [28].

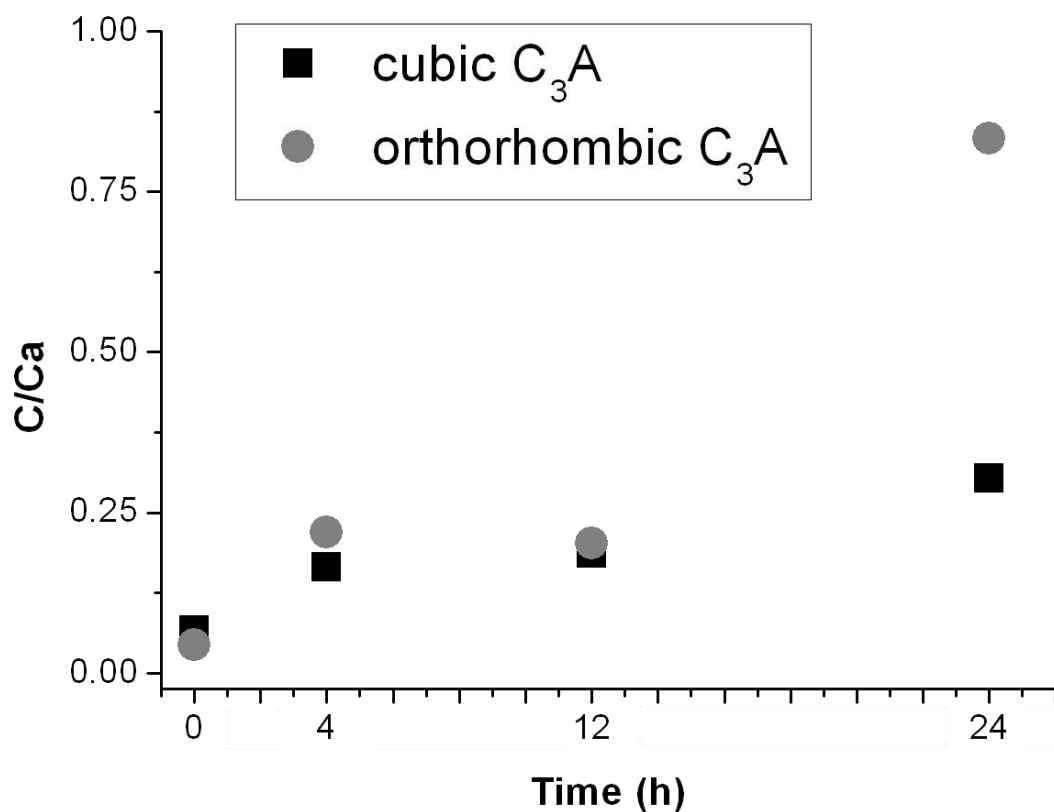
266

267 Carbonation of orthorhombic C_3A was more extensive than for the cubic modification.
268 Sample 24c revealed a C/Ca ratio of 0.8 (**Table 4**). This ratio was too high to be explained
269 solely by calcium monocarboaluminate formation, and indicated the presence of another
270 carbonate species.

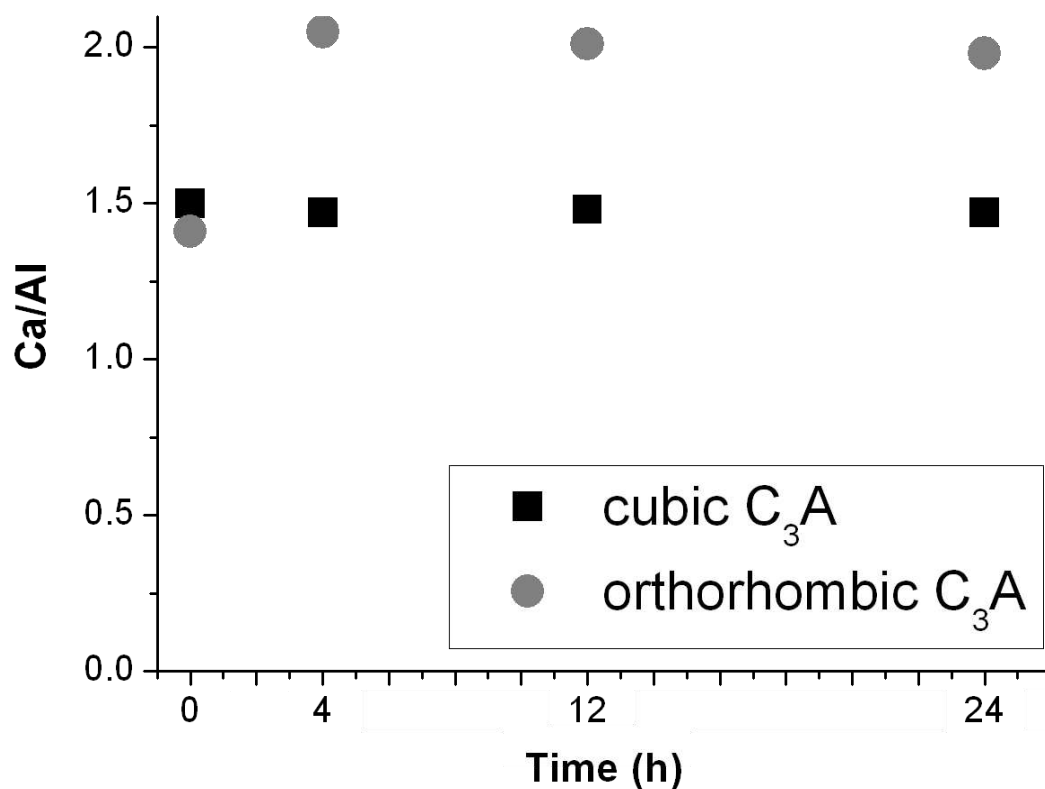
271

272 **Figure 5** shows the changes in C/Ca and Ca/Al ratios with exposure for both C_3A
273 modifications. While there was no change in the Ca/Al ratio of the cubic C_3A , exposure to
274 water vapour led to an increase in Ca/Al ratio for orthorhombic C_3A . We ascribe this to an
275 increase in the surface pH due to surface enrichment in sodium upon prehydration (see
276 below). Such conditions would accelerate the formation of C_4AH_x phases, as observed
277 previously [16]. This may also explain the lower relative humidity threshold above which
278 orthorhombic C_3A begins to prehydrate compared to cubic C_3A [8,15,16].

279



280



281

282 **Fig. 5** Normalised ratios of C/Ca (a) and Ca/Al ratios (b) occurring on the surfaces of cubic

283 and orthorhombic C_3A as a function of ageing period and mode, as measured by XPS

284

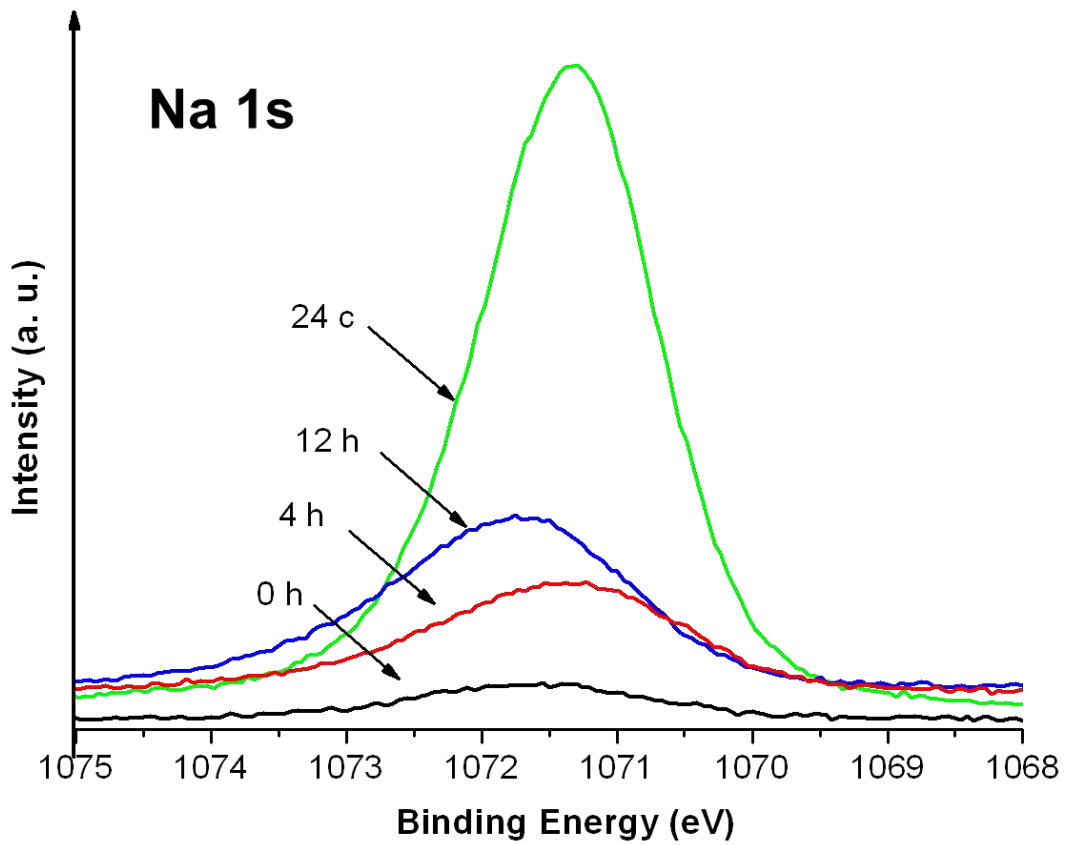
285 3.3 Impact of Na₂O doping

286 The high resolution Na 1s spectra revealed how the presence of sodium affected the reactivity
287 of orthorhombic C₃A, and spectra plus the calculated Na/Ca ratios are shown in **Fig. 6**. The
288 freshly calcined sample exhibited a Na 1s signal comprising of two signals; the main one
289 centred at ~ 1071.5 eV and a second minor peak at ~ 1072.2 eV. No definitive assignment
290 could be made for the major peak, but we assume it to be due to sodium substituted for
291 calcium within the C₃A, while the second peak is of a similar binding energy to the value of
292 1072.3 eV reported for pure Na₂O and NaOH [29,30].

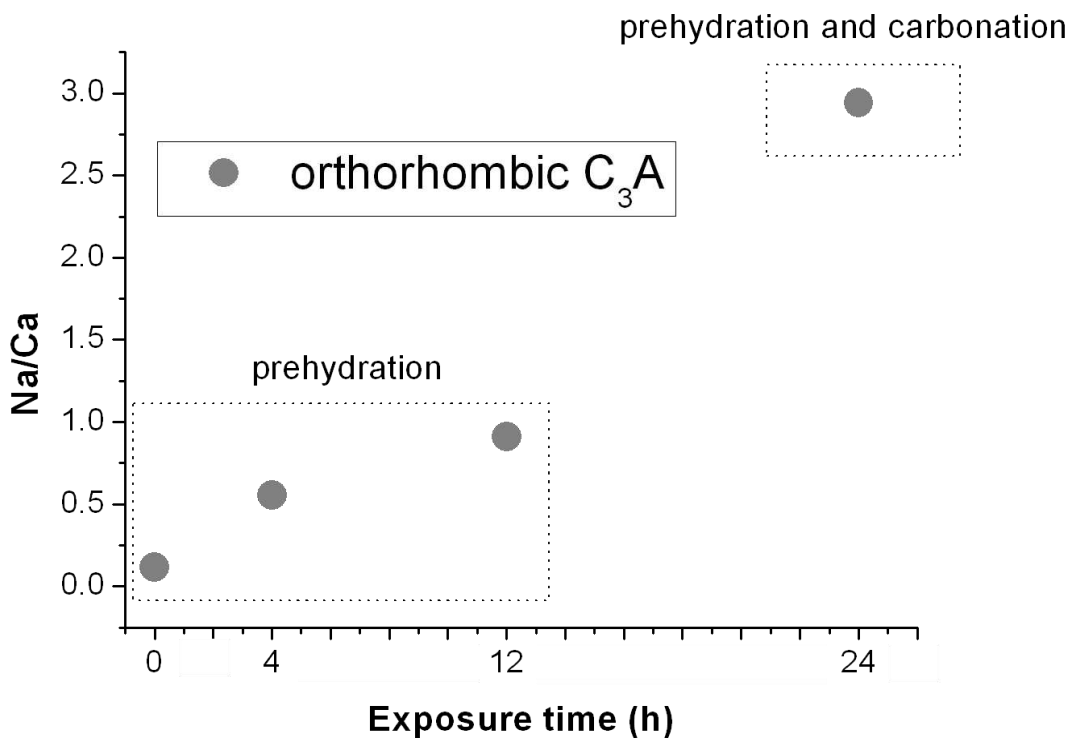
293
294 Exposure to water vapour only led to a gradual increase in the intensity of the signal centred
295 at ~ 1072.2 eV; indicating that less and less sodium was bound within the crystal structure of
296 orthorhombic C₃A, with the increased intensity due to mobilisation of sodium and its
297 migration to the sample surface. This finding agrees with results from Glasser et al. who
298 observed that Na⁺ can dissolve into the aqueous phase more rapidly than Ca²⁺ or Al³⁺ [5].
299 Upon abstraction from the crystal structure, sodium appears to combine with water to form
300 NaOH on the surface, with a binding energy of 1072.2 eV characteristic of NaOH [29].

301
302 Exposure to CO₂ within ambient air led to further changes in the Na 1s spectra, namely a
303 large growth in intensity and a slight shift back to lower binding energies, with the signal
304 centred at 1071.3 eV. Such binding energy may correspond to either Na₂CO₃ or NaHCO₃,
305 both of which produce a peak at 1071.3 eV [29]. This finding suggests that the initially
306 formed NaOH then carbonated to form Na₂CO₃ or NaHCO₃, which constitutes the main
307 product from the prehydration and carbonation process. The formation of this phase also helps
308 to explain the high C/Ca ratio reported above.

309



310



311

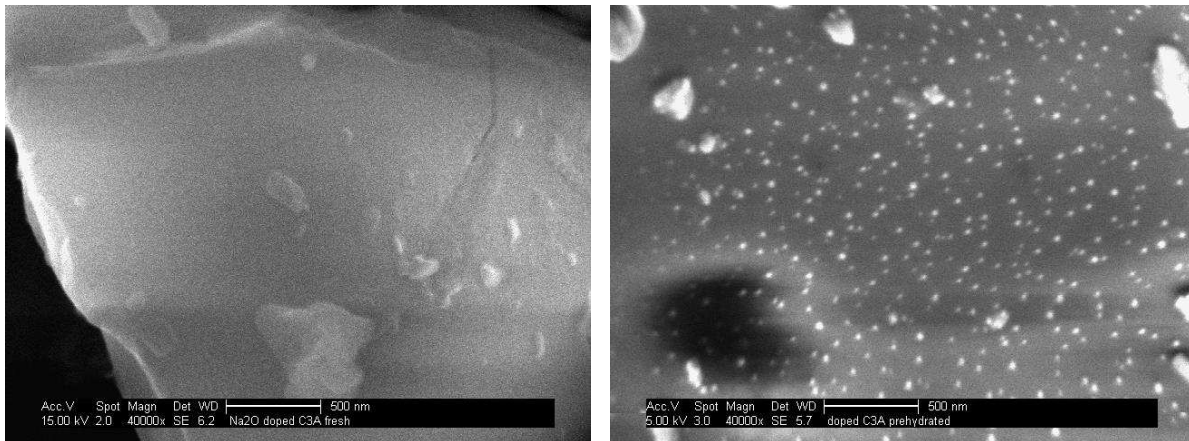
312

313 **Fig. 6** Na 1s XPS spectra of fresh and aged orthorhombic C_3A samples (a) and Na/Ca ratios

314 after exposure of orthorhombic C_3A sample to moisture and CO_2 in air (b)

315

316 The formation of Na_2CO_3 or NaHCO_3 on the surface of o- C_3A was confirmed by SEM
317 imaging (Fig. 7). Bright crystalline specks were visible on the surface of sample 24c, which
318 EDX spectroscopy indicated as comprising of sodium, carbon and oxygen, presumably of
319 Na_2CO_3 or NaHCO_3 .
320



322 **Fig. 7** SEM images of the surfaces of a) 0h (fresh) and b) 24c (prehydrated and carbonated)
323 orthorhombic C_3A , showing Na_2CO_3 or NaHCO_3 crystals on the prehydrated sample.
324

325 4. Conclusions

326 X-ray photoelectron spectroscopy has been used to follow the interactions of cubic and
327 orthorhombic C_3A polymorphs with environmental moisture and CO_2 under defined storage
328 conditions.
329

330 In the XPS spectra, clear differences were observed for cubic and orthorhombic C_3A after
331 prehydration with water vapour and subsequent carbonation in air. During prehydration in the
332 absence of CO_2 , both C_3A polymorphs showed the formation of C_4AH_{13} on their surfaces, but
333 the extent was more pronounced for the orthorhombic polymorph. Surface enrichment of
334 sodium, in the form of sodium hydroxide, was observed after prehydration of orthorhombic
335 C_3A which was doped with 4 wt. % of Na_2O . The increased pH induced by the formation of
336 surface NaOH during prehydration may account for the increased rate of reaction, as has been

337 reported previously [21]. It may also explain why the effects of prehydration become evident
338 at 55% RH for orthorhombic C₃A, but at 80% RH for cubic C₃A [8,16].

339

340 Additionally, the impact of sodium on carbonation of orthorhombic C₃A was studied.
341 Prehydrated cubic C₃A produced monocarboaluminate (3 CaO·Al₂O₃·CaCO₃·11H₂O) on its
342 surface, while carbonation of orthorhombic C₃A resulted in formation of the same phase,
343 together with extensive Na₂CO₃ or NaHCO₃ formation. The reason for the latter is the high
344 amount of NaOH formed after the initial prehydration at the surface of orthorhombic C₃A.

345

346 **Acknowledgments**

347 E. Dubina is grateful to Nanocem (Core Project # 7) for financial support of this work. The
348 authors also like to acknowledge the support from EPSRC (grant reference EP/E025722/1) for
349 supporting this work through the Daresbury NCESS Facility. They also want to thank Dr.
350 Danny Law for his support at NCESS. Additionally, Dr. Holger König and Dr. Maciej Zajac,
351 both from HeidelbergCement, Leimen, Germany are thanked for their input during many
352 discussions.

353

354 **References**

355 [1] H. F. W. Taylor, Cement Chemistry, Academic Press, London, 1990.

356 [2] A. I. Boikova, A. I. Domansky, V. A. Paramonova, G. P. Stavitskaja and V. M.
357 Nikuschenko, "The influence of Na₂O on the structure and properties of 3CaO·Al₂O₃",
358 Cem. Concr. Res. 7, 1977, 483 – 492.

359 [3] L. Gobbo, L. Sant'Agostino, L. Garcez, "C₃A polymorphs related to industrial clinker
360 alkalies content", Cem. Concr. Res. 34, 2004, 657 – 664.

- 361 [4] D. Stephan, H. Maleki, D. Knöfel, B. Eber, R. Härdtl, Influence of Cr, Ni, and Zn on the
362 properties of pure clinker phases: Part II. C_3A and C_4AF , *Cem. Concr. Res.* 29, 1999, 651
363 – 657.
- 364 [5] F. P. Glasser, M. B. Marinho, “Early stages of the hydration of tricalcium aluminate and
365 its sodium containing solid solutions”, *Br. Ceram. Proc.* 35, 1984, 221 – 236.
- 366 [6] S. Wistuba, D. Stephan, G. Raudaschl-Sieber, J. Plank, "Hydration and hydration products
367 of two-phase Portland cement clinker doped with Na_2O ", *Adv. Cem. Res.* 19, 2007, 125 –
368 131.
- 369 [7] A. P. Kirchheim, V. Fernández-Altable, P. J. M. Monteiro, D. C. C. Dal Molin, “Analysis
370 of cubic and orthorhombic C_3A hydration in presence of gypsum and lime”, *J. Mater. Sci.*
371 44, 2009, 2038 – 2045.
- 372 [8] E. Dubina, J. Plank, L. Black and L. Wadso, Impact of environmental moisture on C_3A
373 polymorphs in the absence and presence of $CaSO_4 \cdot 0.5 H_2O$, *Adv. Cem. Res.*, 26(1), 29-40
- 374 [9] H. Pöllmann, Composition of cement phases. In *Structure and Performance of Cements*
375 (BENSTED J. and BARNES P. (eds.)). Spon Press, London, 2002, 25 – 56.
- 376 [10] P. Mondal, and J.W. Jeffery, "The crystal structure of tricalcium aluminate $Ca_3Al_2O_6$ ",
377 *Acta Cryst. B* 31, 1975, 689 – 697.
- 378 [11] C. Ostrowski, J. Żelazny, “Solid Solutions of Calcium Aluminates C_3A , $C_{12}A_7$ and CA
379 with Sodium Oxide”, *J. Therm. Anal. Calorim.*, 75 (3), 2004, 867 – 885.
- 380 [12] E. Breval, “Gas-phase and liquid-phase hydration of C_3A ”, *Cem. Concr. Res.* 7, 1977,
381 297 – 304.
- 382 [13] K. Theisen, V. Johansen, “Prehydration and strength development of Portland cement”,
383 *J. Am. Cer. Soc.*, 54 (9), 1975, 787 – 791.
- 384 [14] M. Whittaker, E Dubina, F Al-Mutawa, L Arkless, J Plank and L Black, “The effect of
385 prehydration on the engineering properties of CEM I Portland cement”, *Adv. Cem. Res.*.
386 25 (1). 2013, 12 - 20.

- 387 [15] E. Dubina, L. Wadsö, J. Plank, “A sorption balance study of water vapour sorption on
388 anhydrous cement minerals and cement constituents”, *Cem. Concr. Res.* 41, 2011, 1196 –
389 1204.
- 390 [16] E. Dubina, L. Black, R. Sieber, J. Plank, “Interaction of water vapour with anhydrous
391 cement minerals”, *Adv. Appl. Ceram.*, 109 (5), 2010, 260 – 268.
- 392 [17] J. T. Grant and D. Briggs “Surface Analysis by Auger and X-ray Photoelectron
393 Spectroscopy”, published by IM Publications, 2003, Chichester, UK.
- 394 [18] L. Greenspan, “Humidity Fixed Points of Binary Saturated Aqueous Solutions”, *J. Res.*
395 *Nat. Bur.*, 8 (1), 1977, 89 – 95.
- 396 [19] C. D. Wagner, L. E. Davis, M. V. Zeller, J. A. Taylor, R. H. Raymond, L. H. Gale,
397 “Empirical atomic sensitivity factors for quantitative analysis by electron spectroscopy
398 for chemical analysis”, *Surf. Interface Anal.*, 3 (5), 1981, 211 – 225.
- 399 [20] L. Black, K. Garbev, I. Gee, “Surface carbonation of synthetic C-S-H samples: A
400 comparison between fresh and aged C-S-H using X-ray photoelectron spectroscopy”,
401 *Cem. Concr. Res.*, 38, 2008, 745 – 750.
- 402 [21] M. C. Ball, R. E. Simmons and I. Sutherland, “Surface composition of anhydrous
403 tricalcium aluminate and calcium aluminoferrite”, *J. Mater. Sci.*, 22, 1987, 1975 – 1979.
- 404 [22] T. L. Barr, S. Seal, K. Wozniak, J. Klinowski, “ESCA studies of the coordination state of
405 aluminium in oxide environments”, *J. Chem. Soc., Faraday Trans.*, 93, 1997, 181 – 186.
- 406 [23] L. Black, A. Stumm, K. Garbev, P. Stemmermann, K. R. Hallam, G. C. Allen, “X-ray
407 Photoelectron Spectroscopy of Aluminium-Substituted Tobermorite”, *Cem. Conc. Res.* ,
408 35 (1), 2005, 51-55.
- 409 [24] Y. Takeuchi, F. Nishi, I. Maki, “Crystal-chemical characterization of the tricalcium
410 aluminate-sodium oxide ($3\text{CaO} \times \text{Al}_2\text{O}_3\text{-Na}_2\text{O}$) solid solution series”, *Z. Kristallogr.* 152
411 (3-4), 1980, 259 – 307.

- 412 [25] L. Black, K. Garbev, G. Beuchle, P. Stemmermann, D. Schild, “X-ray photoelectron
413 spectroscopic investigation of nanocrystalline calcium silicate hydrates synthesised by
414 reactive milling”, *Cem. Concr. Res.*, 36, 2006, 1023 – 1031.
- 415 [26] L. Black, C. Breen, J. Yarwood, J. Phipps and G. Maitland, “In situ Raman analysis of
416 hydrating C₃A and C₄AF pastes in presence and absence of sulphate”, *Adv. Appl. Ceram.*,
417 2006, 105, 209 – 216.
- 418 [27] R. Fischer, H.J. Kuzel, “Reinvestigation of the system C₄A · nH₂O – C₄A · CO₂ · nH₂O”
419 *Cem. Concr. Res.*, 12, 1982, 517 – 526.
- 420 [28] R. Gabrovšek, T. Vuk, V. Kaučič, “The Preparation and Thermal Behavior of Calcium
421 Monocarboaluminate”, *Acta Chim. Slov.*, 55, 2008, 942 – 950.
- 422 [29] J. F. Moulder, W.F. Stickle, P.E. Sobol, K.D. Bomben, in: J. Chastain (Ed.), *Handbook*
423 *of X-Ray Photoelectron Spectra – A Reference Book of Standard Spectra for*
424 *Identification and Interpretation of XPS Data*, Perkin-Elmer, Eden Prairie, Minnesota,
425 1992, p. 229.
- 426 [30] R. A. Zarate, S. Fuentes, J. P. Wiff, V. M. Fuenzalida, A. L. Cabrera, “Chemical
427 composition and phase identification of sodium titanate nanostructures grown from titania
428 by hydrothermal processing”, *J Physics Chemistry Solids*, 68, 2007, 628 – 637.